

Supporting information for

Porous carbon derived from metal-organic framework@graphene quantum dots as electrode materials for supercapacitors and lithium-ion batteries

Hui Yu,^a Wenjian Zhu,^a Hu Zhou,^b Jianfeng Liu,^{*,c} Zhen Yang,^c Xiaocai Hu,^c Aihua Yuan,^{*,a,d}

^a School of Environmental and Chemical Engineering, Jiangsu University of Science and Technology, Zhenjiang 212003, China. E-mail: aihua.yuan@just.edu.cn.

^b School of Material Science and Engineering, Jiangsu University of Science and Technology, Zhenjiang 212003, China.

^c Shanghai Waigaoqiao Shipbuilding Co., LTD, Shanghai 200137, China.

^d Marine Equipment and Technology Institute, Jiangsu University of Science and Technology, Zhenjiang 212003, China.

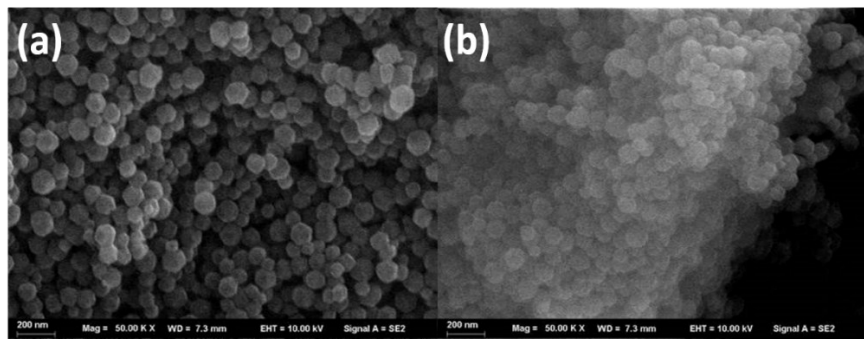


Fig. S1 SEM images of (a) ZIF-8 and (b) ZIF-8@GQDs.

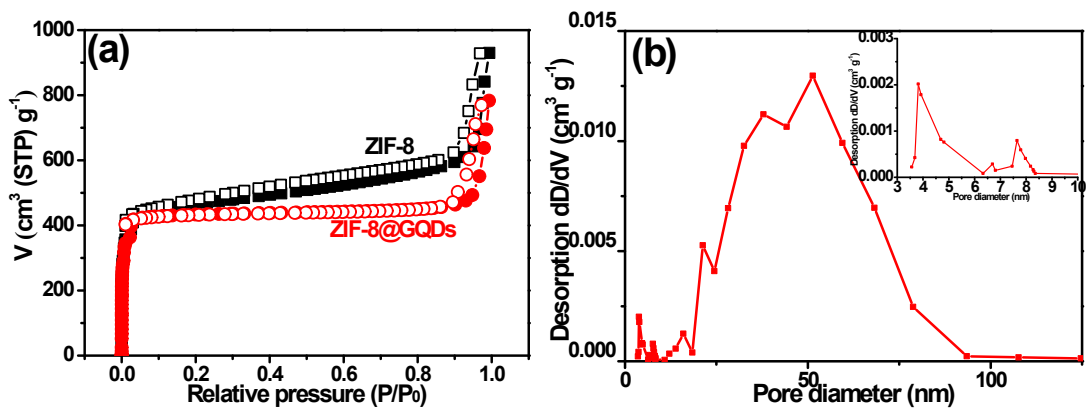


Fig. S2 (a) The N_2 adsorption-desorption isotherm of ZIF-8 and ZIF-8@GQDs; (b) pore size distribution of ZIF-8

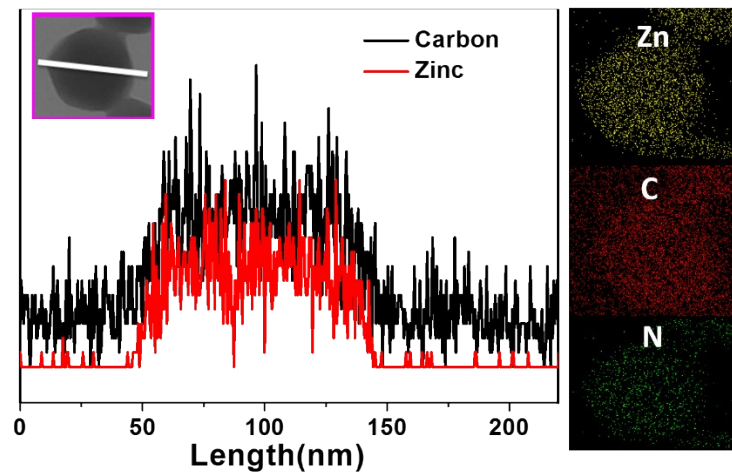


Fig. S3 Elemental line profiles and elemental mapping of ZIF-8@GQDs.

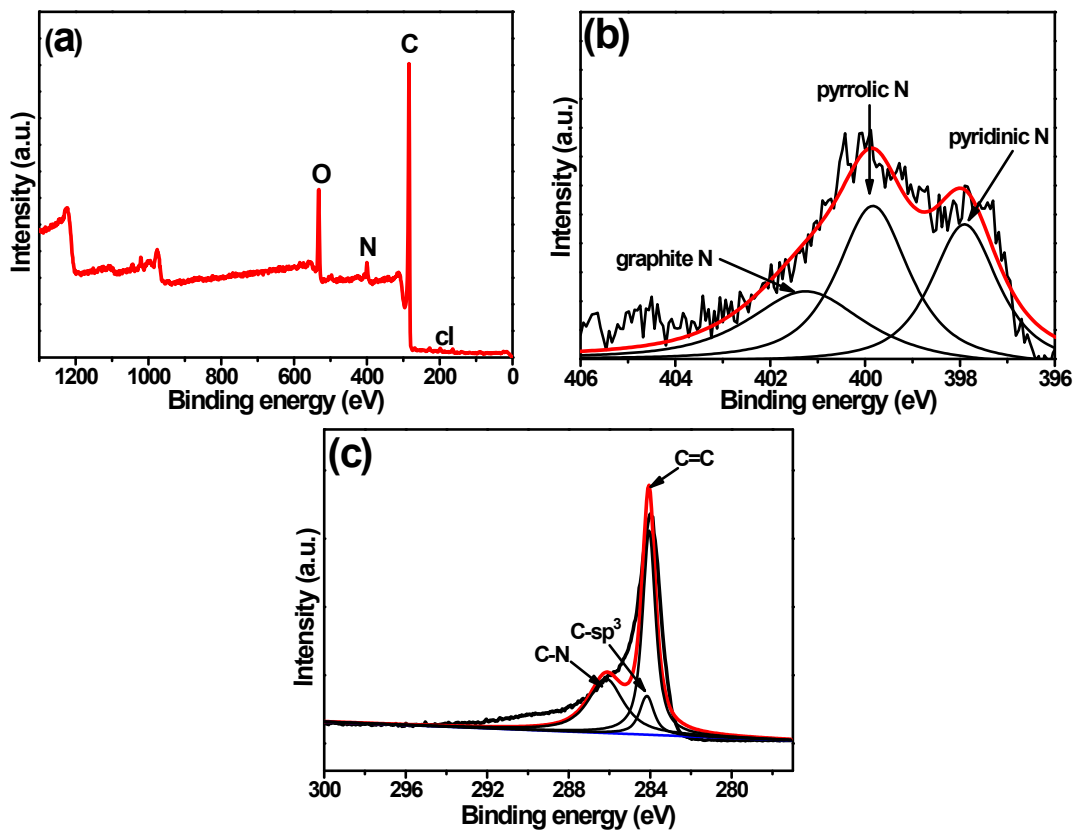


Fig. S4 XPS spectra of C(ZIF-8);(a)survey; (b) N 1s; (c) C 1s.

Table 1 The composition of the obtained porous carbon samples.

C(ZIF-8)@GQDs	XPS (%)						N 1s (%)		
	C	N	O	Zn	cl	graphite N	pyrrolic N	pyridinic N	
	84.58	5.67	8.37	0.53	0.85	49.33	23.64	27.03	
C(ZIF-8)	82.31	5.39	11.78	0	0.53	28.83	38.83	32.33	

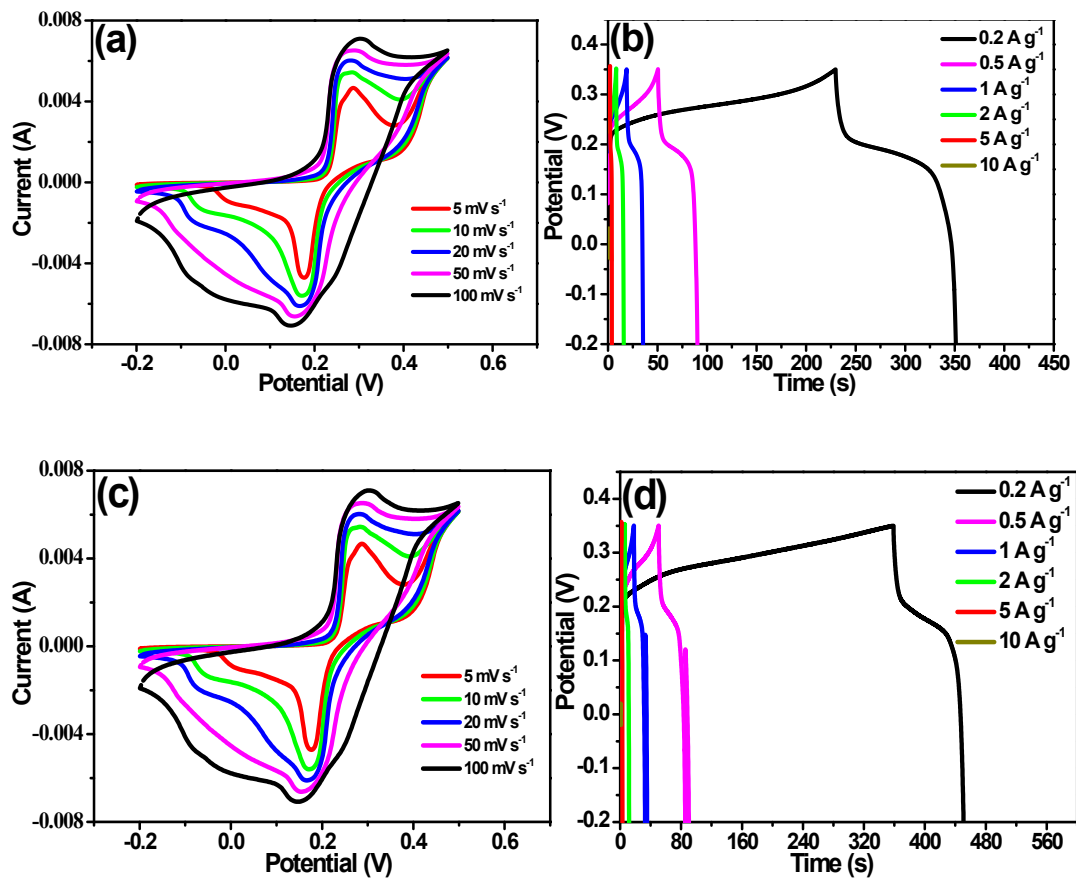
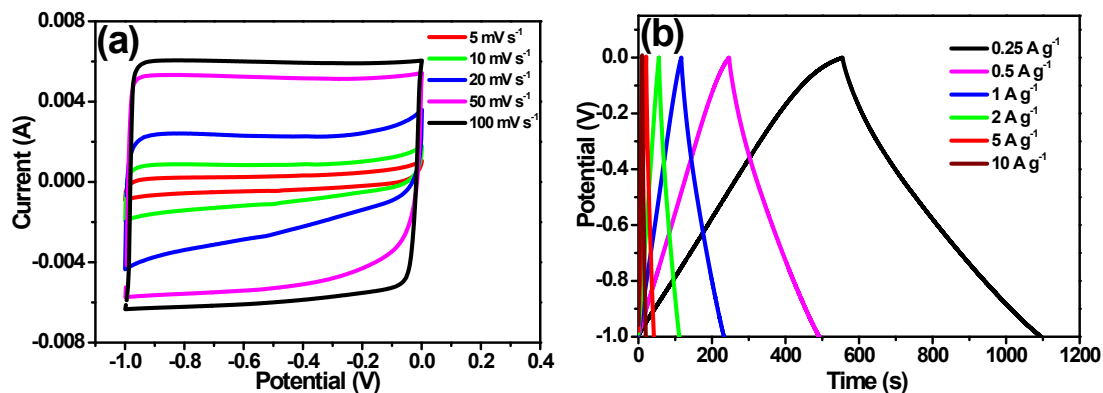


Fig. S5 (a) CV curves of ZIF-8 at different scan rates; (b) GCD curves of ZIF-8 at different current (c) CV curves of ZIF-8@GQDs at different scan rates; (d) GCD curves of ZIF-8@GQDs at different current densities.



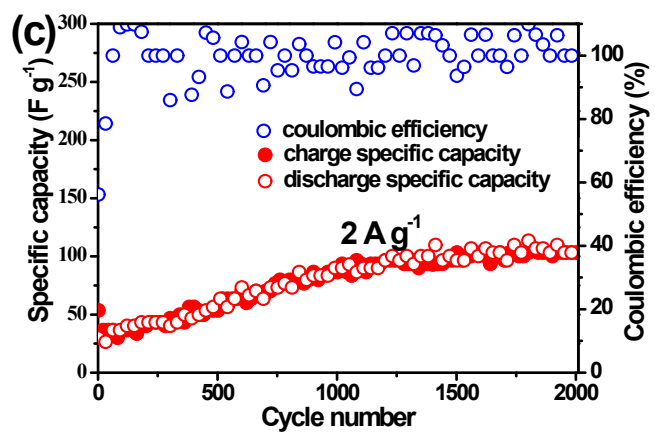


Fig. S6 (a) CV curves of C(ZIF-8) at different scan rates; (b) GCD curves of C(ZIF-8) at different current densities; (c) cycling performance of C(ZIF-8) at 2 A g^{-1} .